

# Atomic Layer Deposition Enabled Interconnect Technology for Vertical Nanowire Arrays

Jen-Hau Cheng<sup>a,d,\*</sup>, Dragos Seghete<sup>b,d</sup>, Myongjai Lee<sup>a,d</sup>, John B. Schlager<sup>c,d</sup>, Kris A. Bertness<sup>c,d</sup>, Norman A. Sanford<sup>c,d</sup>, Ronggui Yang<sup>a,d</sup>, Steven M. George<sup>b,d</sup> and Y. C. Lee<sup>a,d</sup>,

<sup>a</sup> Department of Mechanical Engineering, University of Colorado, Boulder, CO 80309, United States

<sup>b</sup> Department of Chemistry and Biochemistry, University of Colorado, Boulder, CO 80309, United States

<sup>c</sup> National Institute of Standards and Technology, Boulder, Colorado 80305, United States

<sup>d</sup> DARPA Center for Integrated Micro/Nano-Electromechanical Transducers (iMINT), University of Colorado, Boulder, CO 80309-0427, United States

\*Corresponding author: email: Jen-Hau.Cheng@colorado.edu

## Abstract

We have demonstrated an atomic layer deposition (ALD) enabled interconnect technology for vertical, c-axis oriented gallium nitride (GaN) nanowire (NW, 5-10  $\mu\text{m}$  in length, 80-200 nm in diameter) arrays encapsulated by Benzocyclobutene (BCB). The nano-scaled ALD multilayer is essential to provide conformal co-axial dielectric (ALD-alumina)/conductor (ALD-tungsten) coverage and precise thickness control for nanowire metallization. Furthermore, we have successfully developed a fabrication process to locally remove and connect tungsten (W) interconnect on NWs. Cross-sectional image taken in a focused ion beam (FIB) tool confirms the conformality of ALD interconnects. Photoluminescence (PL) wavelengths of the nanowires array can be tuned dynamically by changing the input current supplied to ALD-tungsten interconnect which heats nanowires. Such an experiment also demonstrated the quality of interconnect. This interconnect technology can be applied to various vertical nanowire-based devices, such as nanowire light emitting diodes (LEDs), nanowire-based field effect transistors (FETs), resonators, batteries or biomedical applications.

**Keywords:** Atomic layer deposition (ALD), Interconnect, GaN nanowires, Focused ion beam (FIB), Photoluminescence (PL),

## I. Introduction

Low dimensional materials such as nanowires (NWs) have attracted considerable research attention and interest due to their unique electrical, optical, magnetic properties [1]. They are promising material candidates as fundamental building blocks for future electronic [2,3], optoelectronic [4,5], energy [6], sensor [7] and biomedical [8] applications. Usually NW-based devices are constructed as horizontal configurations. NWs are taken from as-grown substrate, and then assembled, interconnected and tested [9,10]. Vertical nanowire array devices, compared to horizontal NW configurations, are of great importance for achieving ultrahigh integration density at a device level without the need of additional assembly and rearrangement processes. For example, vertical nanowire arrays are the best configuration for solid state super-capacitors [11,12], lithium ion batteries [13] and NW-LEDs [14]. These applications require large surface-to-volume ratio of vertical NWs for enhanced performance and potentially higher efficiency.

Report Documentation Page				Form Approved OMB No. 0704-0188	
Public reporting burden for the collection of information is estimated to average 1 hour per response, including the time for reviewing instructions, searching existing data sources, gathering and maintaining the data needed, and completing and reviewing the collection of information. Send comments regarding this burden estimate or any other aspect of this collection of information, including suggestions for reducing this burden, to Washington Headquarters Services, Directorate for Information Operations and Reports, 1215 Jefferson Davis Highway, Suite 1204, Arlington VA 22202-4302. Respondents should be aware that notwithstanding any other provision of law, no person shall be subject to a penalty for failing to comply with a collection of information if it does not display a currently valid OMB control number.					
1. REPORT DATE <b>JUN 2009</b>		2. REPORT TYPE		3. DATES COVERED <b>00-00-2009 to 00-00-2009</b>	
4. TITLE AND SUBTITLE <b>Atomic Layer Deposition Enabled Interconnect Technology for Vertical Nanowire Arrays</b>				5a. CONTRACT NUMBER	
				5b. GRANT NUMBER	
				5c. PROGRAM ELEMENT NUMBER	
6. AUTHOR(S)				5d. PROJECT NUMBER	
				5e. TASK NUMBER	
				5f. WORK UNIT NUMBER	
7. PERFORMING ORGANIZATION NAME(S) AND ADDRESS(ES) <b>University of Colorado, Department of Mechanical Engineering, Boulder, CO, 80309</b>				8. PERFORMING ORGANIZATION REPORT NUMBER	
9. SPONSORING/MONITORING AGENCY NAME(S) AND ADDRESS(ES)				10. SPONSOR/MONITOR'S ACRONYM(S)	
				11. SPONSOR/MONITOR'S REPORT NUMBER(S)	
12. DISTRIBUTION/AVAILABILITY STATEMENT <b>Approved for public release; distribution unlimited</b>					
13. SUPPLEMENTARY NOTES					
14. ABSTRACT <b>see report</b>					
15. SUBJECT TERMS					
16. SECURITY CLASSIFICATION OF:			17. LIMITATION OF ABSTRACT <b>Same as Report (SAR)</b>	18. NUMBER OF PAGES <b>25</b>	19a. NAME OF RESPONSIBLE PERSON
a. REPORT <b>unclassified</b>	b. ABSTRACT <b>unclassified</b>	c. THIS PAGE <b>unclassified</b>			

Studies have been made on interconnect and integration of vertical NWs. Electrical interconnect to the top of NWs has been demonstrated by using electrostatic attachment of gold nanoparticles onto the tips of NWs [15]. Interconnect is formed from the bottom electrode through NWs to the top gold nanoparticle film. Vertical integration of NWs has been developed by using a sequence of fabrication process from material filling, mechanical polishing to the formation of top and bottom electrical interconnects [16]. Usually, nanowires are parts of interconnects, and electrodes are formed on top and bottom of NWs. For vertical NW-based LEDs, FETs or batteries, device performance could be significantly enhanced through the utilization of the large surface-to-volume ratio of vertical NWs while coated with high-quality electrical and dielectric interconnects. However, it is always a challenge to interconnect these vertical/as-grown nanowires because of their small diameters, extremely high aspect ratios, and random distributions on the substrate. In addition, for certain applications, to locally remove and connect interconnects on vertical NWs is another challenge.

Our study presents a new interconnect technology for vertical NW arrays with a novel nano-scaled conductor/dielectric multilayer fabricated using atomic layer deposition (ALD). Benzocyclobutene (BCB) is employed as filling material to encapsulate NWs. We have also developed a fabrication process to locally remove and connect tungsten interconnect on NWs. Using local interconnect process, we can dynamically tune the wavelength of GaN NWs by heating the NWs via input current supplied to ALD-tungsten interconnect and verify the connection of interconnect.

## **II. Nanowires Interconnected with Tips Covered**

Figure 1 shows the c-axis oriented GaN NWs that were grown on Si (111) in an entirely catalyst free fashion using nitrogen plasma enhanced molecular beam epitaxy (MBE). The detailed synthesis technique could be found in references [17,18]. These wires are defect-free with a typical diameter of 150 nm. The nanowires used in this study were roughly 8  $\mu\text{m}$  in length.

We then employed ALD processes to interconnect GaN NWs. ALD is a low temperature (for example, 120°C for  $\text{Al}_2\text{O}_3$  and W film growth) thin film growth technique allowing atomic-scale thickness control. ALD utilizes a binary reaction sequence of self-limiting chemical reactions between gas phase precursor molecules and a solid surface [19, 20]. Films deposited by ALD are extremely smooth, pinhole-free and conformal to the underlying substrate surface. This conformality enables successful uniform coating of the entire nanowire device. Furthermore, ALD is a low temperature process enabling deposition on thermally sensitive materials.

ALD- $\text{Al}_2\text{O}_3$  (30 nm) and ALD-W (40 nm) were sequentially deposited on the surface of NWs which serves as a dielectric layer and an electrical connection layer, respectively. The conformality of ALD- $\text{Al}_2\text{O}_3$  coating was verified by field emission scanning electron microscopy (FESEM) as shown in Figure 2, from side view and top view (inset). Figure 3 shows the FESEM images of tungsten layers (deposited by ALD and sputtering) and placed on top of the ALD- $\text{Al}_2\text{O}_3$  layer. Apparently, ALD deposition provides a more conformal tungsten coating (Figure 3a) compared to sputtered W (Figure 3b). A polymer

encapsulation process for the interconnected vertical NW devices has also been developed. This encapsulation processing was needed to finalize the interconnect of the devices coated with the ALD conductor/dielectric multilayer and also provide a robust mechanical support. In this study, we selected BCB as the filling material to encapsulate vertical NWs. BCB has been widely adopted in a variety of electronic applications, including silicon and compound semiconductor passivation, interlayer dielectric, flat panel display, IC packaging, integrated passives, MEMS, wafer bonding and 3D integration, and optoelectronic components due to the favorable material properties of BCB such as low dielectric constant (2.65) and low dissipation factor (0.0008) [21]. Several droplets of BCB were dripped on the NWs chip, and then soft baked at 90°C for 4 minutes, exposed to UV, and then hard baked at 250°C for 1 hour (Figure 4a). To expose the tips of NWs, mechanical polishing was first employed to reduce the thickness of BCB and then plasma reactive ion etching (RIE) was used for selective BCB etching. Figure 4b shows the exposed NW tips. However, as shown in the figure 4b and 4c, polishing process could result in NW tip damage, and also result in residual voids and cavities between the BCB and the NWs. Such cavities may electrically isolate the NW tip from the top conducting surface.

To eliminate these cavities, a second ALD-W (30 nm) coating was introduced to assure a conformal conductor coating that would cover every NW tip even down and into the cavities. This ALD conductor coating is followed by a thick top W electrode which is deposited by sputtering with a thickness of 170 nm. As a result, a continuous electrical interconnection from top tips of NWs through the surface of NWs to the bottom substrate is formed. We note that the top electrode can be patterned to interconnect a specific number of NWs. This ALD-enabled interconnection scheme is of critical importance for the development of core-sleeve vertically aligned NW LEDs. In other potential applications of nanowire structures, such as supercapacitors, the ALD-alumina dielectric layer may also play an important role. Figure 5 reveals the detail of the layer-by-layer structure using Focused-Ion-Beam (FIB) cross-sectional cutting. The conformal ALD- $\text{Al}_2\text{O}_3$  / ALD-W layers on the NWs, and the second ALD-W layer to fill the voids/cavities described earlier are shown in the figure.

### **.III. Nanowires Interconnected with Tips Exposed**

For vertical NW-based LEDs or lasers, tip regions of NWs are the passages of light output. Light output could be blocked by the design of a whole surface of metal interconnect on top of encapsulation material and NWs. For NW-based FETs, gate interconnect need to be separated from source and drain interconnects. Apparently a local interconnect process to connect NW-based devices is essential to many practical applications. In order to demonstrate the capability of fabricating specific NW-based device configurations by using ALDs as interconnects, we have successfully developed a fabrication process to locally remove metal layer at tip region of NWs. With local interconnect process, ALD-W could provide current injections on NW-based devices while ALD-W at NW tip region is locally removed. These nanowire array devices could then be tested electro-optically as described in Section IV. Figure 6 shows the schematic drawing of NWs interconnected with tip covered (6a), and with tips exposed (6b) after the local interconnect process.

The goal of the local interconnect process is to remove the W metallization layer on tips of NWs. Figure 7 shows the detailed schematic process flow and corresponding experimental results. No photolithography mask is needed in this process. The process starts with as-grown GaN NWs (Fig.7a) coated with ALD- $\text{Al}_2\text{O}_3$  and W (Fig.7b). Fig. 7b shows a cross-sectional image of ALD- $\text{Al}_2\text{O}_3$  and W on a NW. SEM image was taken at the edge of a NW chip cut from a NW wafer. The NW was broken due to the cutting force. Again,  $\text{Al}_2\text{O}_3$  and W grown by ALD method are conformal. To improve the wettability of NW surfaces, oxygen plasma treatment of 20 seconds was conducted before BCB spin-coating on NW sample. Next, tips of NWs were exposed by selective RIE etching (Fig.7c) and ALD-W at tips was removed by W-etchant. ALD- $\text{Al}_2\text{O}_3$  is a good passivation layer and can sustain W-etching process. By controlling the etching time, length of W removal at tips can be controlled. We observed the local W removal at tips after further BCB etching by RIE (Fig.7d). Top W interconnect was made by first a thin ALD-W layer (36nm) for making sure that all NWs are covered and interconnected, and then a thick sputtered-W layer (110nm) (Fig.7e). Then, BCB was spun on the sample again. Tips of NWs were exposed by RIE and W (ALD-W and sputtered-W) at tips was removed by W-etchant (Fig.7f). The etching time is critical not only to control the length of W interconnect at tip to be removed, but also not to cut off the top interconnect between NWs. Finally, BCB was removed by RIE as shown in Figure 8. The ALD-W on NWs are electrically interconnected and W on tips is removed (Fig.8). In local interconnect process, BCB was spun on NW sample, not by dripping. Thick BCB is not desirable because mechanical polishing process is required to reduce the thickness of BCB. Using BCB spin coating, thickness of BCB can be controlled by the ramping and spinning speed. Thus, polishing process can be eliminated if BCB is thin. Since we have eliminated mechanical polishing process, we don't need to worry about the possibility of NW damage. Cavity issue can also be improved by oxygen plasma treatment before BCB spin coating.

#### **IV. Tuning GaN Nanowire Bandgaps by Heating**

Wavelength controllability is important for applications of laser and LEDs. Previous studies focused on tuning NW bandgap by changing material compositions [22,23]. Changing the material properties from material itself is one way; applying an external pressure, temperature or electrical field could result in a dynamic tuning of the bandgaps. In our study, we demonstrate the dynamic tuning of GaN nanowire bandgaps by heating the NWs through ALD-W interconnect. With current injection to ALD-tungsten interconnect, the connection quality of ALD-W interconnect along NWs can also be verified by this bandgap tuning demonstration. ALD-W interconnect is locally heated due to joule heating when current passes through. As a result, the NWs are heated. As the temperature of a semiconductor increases, the lattice expands and then leads to a change of energy bandgap [24]. We used photoluminescence (PL) system to characterize the dynamic tuning of GaN nanowires bandgap [25,26]. Since W on tips of NWs was removed by local interconnect process, PL light can be generated and measured from the tips. PL signals are from the tips of the NWs, and verified by spatially-resolved and steady-state PL measurements to be published in another paper. PL signals are tuned by changing the power input supplied to ALD-W on NWs. To control the direction of current flow in ALD-W along the surface of NWs, two metal pads were made by FIB

machining as shown in Figure 9. As illustrated in Figure 9a, metal pads 1 and 2 are separated by FIB machined trenches but electrically connected through the ALD-W interconnect on NWs and the NW base region.

Figure 10 shows the experimental setup of PL measurement. NW sample is placed on a thermoelectric device (TEC) (functioning as a substrate heater) and excited with a continuous-wave (CW) HeCd laser operating at 325 nm (3.815eV). A K-type thermocouple is placed on the TEC to monitor the surface temperature of the TEC. Two electrical probes were respectively positioned and located at the metal pads machined by FIB using microscope. Figure 11 shows the PL measurement results with/without injecting current into ALD-W interconnect. We first change TEC temperature to tune PL peak wavelength (solid line in blue). This shift can also be achieved by heating the same NWs sample via current injection into ALD-W interconnect as shown in the figure (dash line in red). Red-shifted PL spectrum is observed with power input of 1637mW into ALD-W interconnect. Bandgap of GaN NW is changed due to the temperature increase by power input into ALD-W interconnect, thus changing the PL peak wavelength. The connection of ALD-W interconnect is also verified by PL measurement with injecting current. We also note that there is slightly change of the PL slope for different heating mechanisms (TEC heating or current injection) which could be due to the non-uniformity of the temperature distribution along the NWs. More PL tuning results are shown in figure 12. In experiment, temperature dependence of PL peak wavelength was first measured. We change the input power of the TEC and record PL signals at different TEC temperatures. There is no power input into ALD-W interconnect via electrical probes. It should be noted that PL peak wavelength is determined by using the quadratic fit to the neighboring data of raw peak. At one TEC temperature condition we record 6 measurements and make one error bar with one standard deviation. Afterward, we start to inject current into ALD-W interconnect on NWs via probes and tune the PL peak wavelengths. In figure 12, two target wavelengths, 368nm and 366.04nm, were chosen when surface temperatures of the TEC were 88°C and 55.5°C, respectively. At lower temperature conditions of the TEC (27.3°C and 38.8°C), we start to heat NWs by injecting current into ALD-W interconnect on NWs. By changing the input current supplied to ALD-W interconnect, PL peak wavelengths were tuned to our targets. The only flowing path for injected current is first from pad\_1 through the ALD-W interconnect on NWs to the base region, and then flow back from base region to pad\_2 through ALD-W interconnect on NWs. Tunable GaN NWs by heating demonstrates a feasible method to fast tune bandgap of GaN NWs. Also, this heating effect is also important to the NW-based devices with interconnect along NWs.

## V. Conclusions

We have demonstrated an ALD-enabled interconnect technology for vertical nanowire arrays. The nano-scaled conductor/dielectric multilayer is essential to the interconnect technology. FESEM images and cross-sectional image by FIB confirm the conformal ALD- $\text{Al}_2\text{O}_3$  and W layer along the GaN NWs with high aspect ratio. We have also developed a fabrication process to locally remove and connect W interconnect on NWs. By injecting current into W interconnect along NWs, PL wavelengths can be tuned dynamically by changing input current. PL tuning experiment also verifies the connection of interconnect on NWs. This interconnect technology can be applied to various vertical

nanowire-based devices, such as nanowire light emitting diodes (LEDs), nanowire-based field effect transistors (FETs), resonators, batteries or biomedical applications.

### **Acknowledgements**

The studies conducted by the authors from the University of Colorado-Boulder are supported by the DARPA Center on Nanoscale Science and Technology for Integrated Micro/Nano-Electromechanical Transducers (iMINT) funded by DARPA/MEMS S&T Fundamentals Program (HR0011-06-1-0048)(Dr. D. L. Polla, Program Manager) and another DARPA grant for “Enabling System Integration Technologies for NW-Enabled LED Microsystems” (W31P4Q-08-1-0014). The authors also thank Nanomaterials Characterization Facility (NCF) at University of Colorado-Boulder for the use of FESEM and FIB.

### **References**

- [1] Joondong Kim, and Wayne A. Anderson “Direct Electrical Measurement of the Self-Assembled Nickel Silicide Nanowire”, *Nano Lett.*, 2006, 6 (7), 1356-1359.
- [2] Tomas Bryllert, Lars-Erik Wernersson, Truls L'owgren and Lars Samuelson, “Vertical wrap-gated nanowire transistors”, *IEEE Nanotechnology* 17 (2006) S227–S230.
- [3] Volker Schmidt, Heike Riel, Stephan Senz, Siegfried Karg, Walter Riess, and Ulrich Gçsele, “Realization of a Silicon Nanowire Vertical Surround-Gate Field-Effect Transistor”, *small* 2006, 2, No. 1, 85 – 88.
- [4] Fang Qian, Silvija Gradecak, Yat Li, Cheng-Yen Wen, and Charles M. Lieber, “Core/Multishell Nanowire Heterostructures as Multicolor, High-Efficiency Light-Emitting Diodes”, *Nano Lett.*, Vol. 5, No. 11, 2005.
- [5] Hwa-Mok Kim, Tae Won Kang and Kwan Soo Chung, “Nanoscale Ultraviolet-Light-Emitting Diodes Using Wide-Bandgap Gallium Nitride Nanorods”, *Adv. Materi.* 2003, 15, No. 7-8.
- [6] Candace K. Chan, Hailin Peng, Gao Liu, Kevin McIlwrath, Xiao Feng Zhang, Robert A. Huggins and Yi Cui, “High-performance Lithium Battery Anodes Using Silicon Nanowires”, *Nature Nanotechnology* 3, 31 - 35 (2008).
- [7] Mingwei Li, Rustom B. Bhiladvala, Thomas J. Morrow, James A. Sloss, Kok-Keong Lew, Joan M. Redwing, Christine D. Keating and Theresa S. Mayer, “Bottom-up Assembly of Large-Area Nanowire Resonator Arrays”, *Nature Nanotechnology* 3, 88 - 92 (2008).
- [8] Inkyu Park, Zhiyong Li, Albert P. Pisano, and R. Stanley Williams, “Selective Surface Functionalization of Silicon Nanowires via Nanoscale Joule Heating”, *Nano Lett.*, Vol. 7, No. 10, 2007.
- [9] M. Saif Islam, S. Sharma, T.I. Kamins and R. Stanley Williams, “A Novel Interconnection Technique for Manufacturing Nanowire Devices”, *Appl. Phys. A* 80, 1133–1140 (2005).
- [10] Song Jin, Dongmok Whang, Michael C. McAlpine, Robin S. Friedman, Yue Wu and Charles M. Lieber, “Scalable Interconnection and Integration of Nanowire Devices without Registration”, *Nano Lett.*, Vol. 4, No. 5, 2004.

- [11] Stefano Roddaro, Kristian Nilsson, Gvidas Astromskas, Lars Samuelson, Lars-Erik Wernersson, Olov Karlström, and Andreas Wacker, "InAs Nanowire Metal-Oxide-Semiconductor Capacitors", *Applied Physics Letters*, 92, 253509, 2008.
- [12] T. Mårtensson, J. B. Wagner, E. Hilner, A. Mikkelsen, C. Thelander, J. Stangl, B. J. Ohlsson, A. Gustafsson, E. Lundgren, L. Samuelson, and W. Seifert, "Epitaxial Growth of Indium Arsenide Nanowires on Silicon Using Nucleation Templates Formed by Self-Assembled Organic Coatings" *Adv. Mater. (Weinheim, Ger.)* 19, 1801 2007.
- [13] Candace K. Chan, Hailin Peng, Gao Liu, Kevin McIlwrath, Xiao Feng Zhang, Robert A. Huggins and Yi Cui, "High-performance Lithium Battery Anodes Using Silicon Nanowires", *Nature Nanotechnology* 3, 31 – 35, 2008.
- [14] Myongjai Lee, Jen-Hau Cheng, Y.C. Lee, Dragos Seghete, Steven M. George, John B. Schlager, Kris A. Bertness, Norman A. Sanford, "Packaging and Interconnect Technologies for the Development of GaN Nanowire-Based Light Emitting Diodes", 59<sup>th</sup> Electronic Components and Technology Conference (ECTC), 843-847, 2009.
- [15] Prahalad M Parthangal, Richard E Cavicchi and Michael R Zachariah, "A Universal Approach to Electrically Connecting Nanowire Arrays Using Nanoparticles-Application to A Novel Gas Sensor Architecture", *IEEE Nanotechnology* 17 (2006) 3786–3790.
- [16] E Latu-Romain, P Gilet, P Noel, J Garcia, P Ferret, M Rosina, G Feuillet, F L'evy and A Chelnokov, "A Generic Approach for Vertical Integration of Nanowires", *IEEE Nanotechnology* 19 (2008) 345304.
- [17] K.A. Bertness, A. Roshko, N.A. Sanford, J.M. Barker and A.V. Davydov, "Spontaneously grown GaN and AlGaIn nanowires", *Journal of Crystal Growth* 287 (2006) 522–527.
- [18] K.A. Bertness, N.A. Sanford, J.M. Barker, J.B. Schlager, A. Roshko, A. V. Davydov and I. Levin, "Catalyst-free growth of GaN nanowires", *Journal of Electronic Material*, Vol. 35, No. 4, 2006.
- [19] Elam, J. W. and S. M. George, "Growth of ZnO/Al<sub>2</sub>O<sub>3</sub> alloy films using atomic layer deposition techniques," *Chem. Mater.* 15 (2003), p. 1020.
- [20] S. M. George, A. W. Ott and J. W. Klaus, "Surface Chemistry for Atomic Layer Growth," *Journal of Physical Chemistry*, 100 (1996), pp. 13121-13131.
- [21] CYCLOTENE Advanced Electronic Resins – Processing Procedures for CYCLOTENE 3000 Series for dry etching resins, Feb. 2005 ([www.dow.com/cyclotene](http://www.dow.com/cyclotene)).
- [22] Tevye Kuykendall, Philipp Ulrich, Shaul Aloni and Peidong Yang, "Complete Composition Tunability of InGaIn Nanowires Using a Combinatorial Approach", *Nature materials*, 6, 2007.
- [23] Savarimuthu Philip Anthony, Jeong In Lee, and Jin Kon Kim, "Tuning Optical Band Gap of Vertically Aligned ZnO Nanowire Arrays Grown by Homoepitaxial Electrodeposition", *Appl. Phys. Lett.* 90, 103107, 2007.
- [24] Y. P. Varshni, *Physica* 34, 149 (1967).
- [25] John B. Schlager, Kris A. Bertness, Paul T. Blanchard, Lawrence H. Robins, Alexana Roshko, and Norman A. Sanford, "Steady-state and time-resolved photoluminescence from relaxed and strained GaN nanowires grown by catalyst-free molecular-beam epitaxy", *J. Appl. Phys.* 103, 124309, 2008.

[26] John B. Schlager, Norman A. Sanford, Kris A. Bertness, Joy M. Barker, Alexana Roshko, and Paul T. Blanchard, “Polarization-resolved photoluminescence study of individual GaN nanowires grown by catalyst-free molecular beam epitaxy”, Appl. Phys. Lett. 88, 213106, 2006.

## Figure Captions

Figure 1: Field-emission scanning microscopy (FESEM) image of c-axis oriented GaN nanowires. Nanowires, ranging from 5-10  $\mu\text{m}$  in length and 80-200 nm in diameter, were grown on silicon (111) by nitrogen plasma enhanced MBE [17,18]. The faceted GaN matrix is visible in the image. Inset: top view of single NW (Scale bar: 100nm).

Figure 2: Cross-sectional and top view (inset) SEM images of ALD- $\text{Al}_2\text{O}_3$  layer (30 nm, shell) on GaN NW (core). Conformal  $\text{Al}_2\text{O}_3$  (30 nm) was deposited on the surface of NWs as a dielectric layer using atomic layer deposition. Scale bar: 100 nm.

Figure 3: Tungsten (W) layers deposited on GaN NWs by different coating methods (a) ALD-W (inset: white shell) (b) Sputtered-W. Compared to sputtered W, ALD-W is much smoother and more conformal to the surface of NWs with high aspect ratio (5-10  $\mu\text{m}$  in length and 80-200 nm in diameter). ALD-W layer is used as a metal interconnect for vertical GaN NWs.

Figure 4: BCB encapsulation process for vertical GaN NWs. (a) GaN NWs were buried in thick BCB by dripping. (b) Mechanical polishing was employed to reduce thickness of BCB and tips of NWs were then exposed after RIE process. (c) Schematic drawing of cavity shown in (b). Scale bar in (b): 1 $\mu\text{m}$ .

Figure 5: (a) Cross-sectional view of NW with ALD layers after FIB cutting. Scale bar: 400nm. (b) The corresponding schematic drawing. Second ALD-W was deposited for conformal coverage in the cavities. Sputtered-W with a thickness of 170nm was deposited after second ALD as a thick top electrode.

Figure 6: Schematic drawing of (a) nanowires interconnected with tips covered, and (b) nanowires interconnected with tips exposed after the local interconnect process. Photoluminescence signal can be generated and measured after W at tips is locally removed.

Figure 7: Fabrication process flow and corresponding experimental results of a local interconnect process that results in nanowires interconnected with tips exposed (no W-layer on the NW tip).

Figure 8: (top) Schematic drawing of final step of local interconnect process and (bottom) SEM image of GaN NWs with tip exposed (no W on tip region) after local interconnect process.

Figure 9: (a) SEM image of trenches fabricated by FIB and (b) schematic drawing of cross-sectional view. Trenches were fabricated by FIB cutting to isolate pad 1 and pad 2.

The dimension of each pad is 200um (width) x 100um (length). The depth of trenches is 3um.

Figure 10: Experimental setup of PL measurement. Probes were respectively positioned on pads of NW sample under optical microscope to provide current into W interconnect. The laser spot diameter is around 13um. Average number of NWs shined by laser is 10 by FESEM examination.

Figure 11: Experimental results of PL tuning by using TEC to heat NWs (solid line in blue) and by injecting current into W interconnect to heat NWs (dash line in red). The connection of W interconnect on NWs was confirmed by current injection into W interconnect to tune PL wavelength. The difference in PL slope could be due to the non-uniformity of the temperature distribution along the NWs under different heating mechanisms (TEC heating or current injection).

Figure 12: Experimental results of tunable PL wavelength by heating. PL peak wavelength of NW array can be dynamically tuned to target wavelengths by changing the input power supplied to ALD-tungsten interconnect. PL peak wavelength is determined by using the quadratic fit to the neighboring data of raw peak.

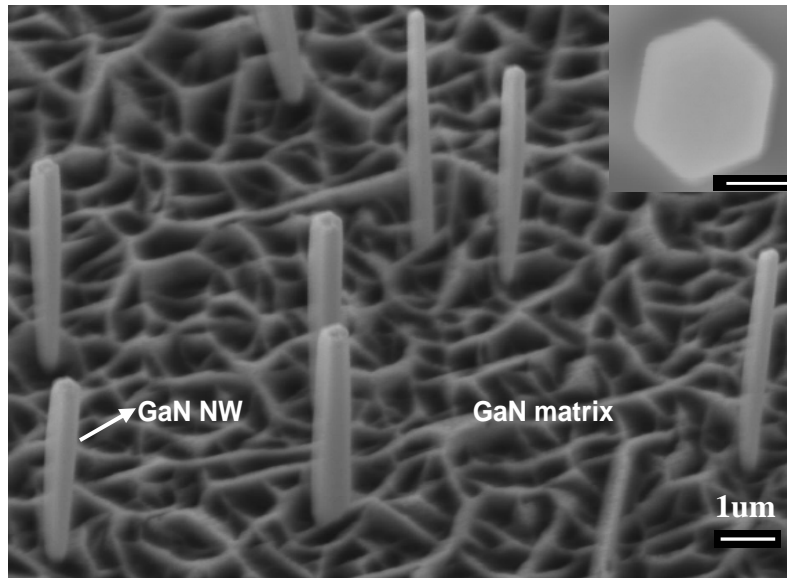


Figure 1: Field-emission scanning microscopy (FESEM) image of c-axis oriented GaN nanowires. Nanowires, ranging from 5-10  $\mu\text{m}$  in length and 80-200 nm in diameter, were grown on silicon (111) by nitrogen plasma enhanced MBE [17,18]. The faceted GaN matrix is visible in the image. Inset: top view of single NW (Scale bar: 100nm).

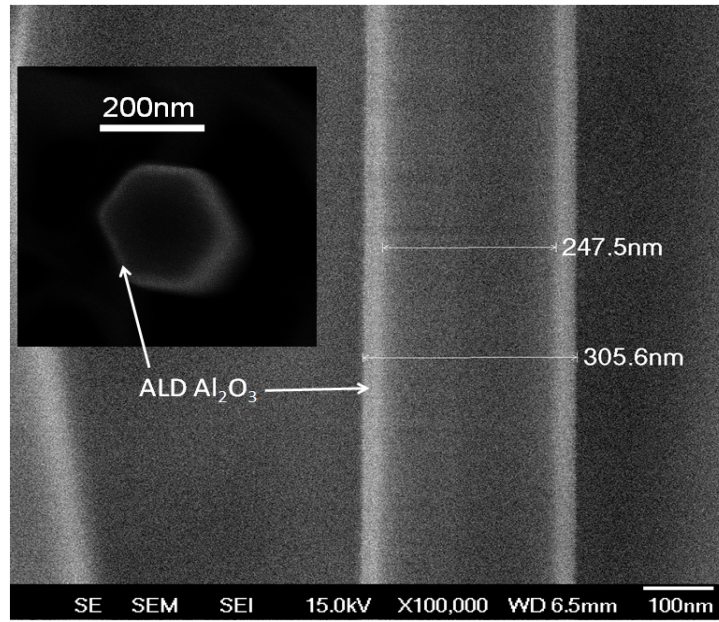


Figure 2: Cross-sectional and top view (inset) SEM images of ALD- $\text{Al}_2\text{O}_3$  layer (30 nm, shell) on GaN NW (core). Conformal  $\text{Al}_2\text{O}_3$  (30 nm) was deposited on the surface of NWs as a dielectric layer using atomic layer deposition. Scale bar: 100 nm.

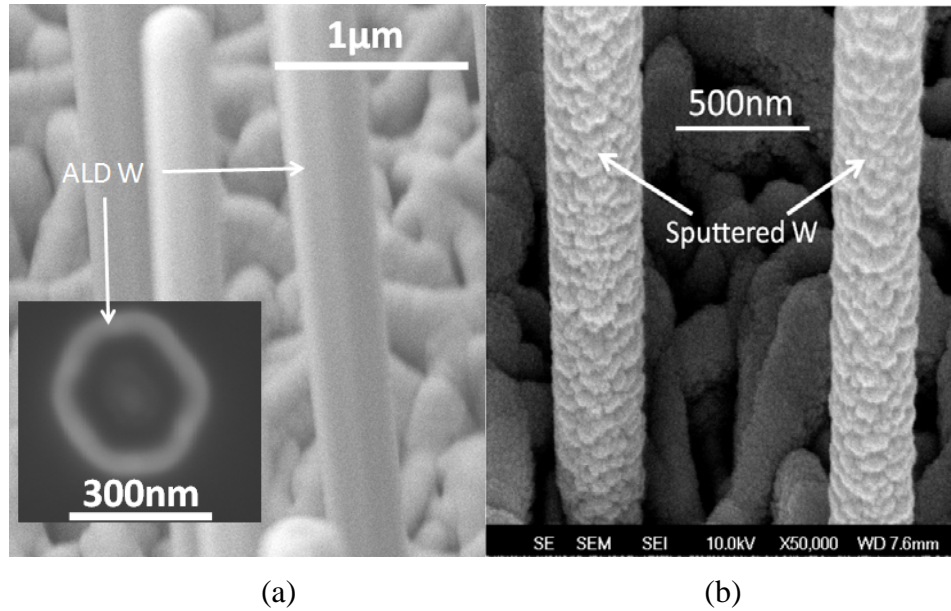


Figure 3: Tungsten (W) layers deposited on GaN NWs by different coating methods (a) ALD-W (inset: white shell) (b) Sputtered-W. Compared to sputtered W, ALD-W is much smoother and more conformal to the surface of NWs with high aspect ratio (5-10  $\mu\text{m}$  in length and 80-200 nm in diameter). ALD-W layer is used as a metal interconnect for vertical GaN NWs.

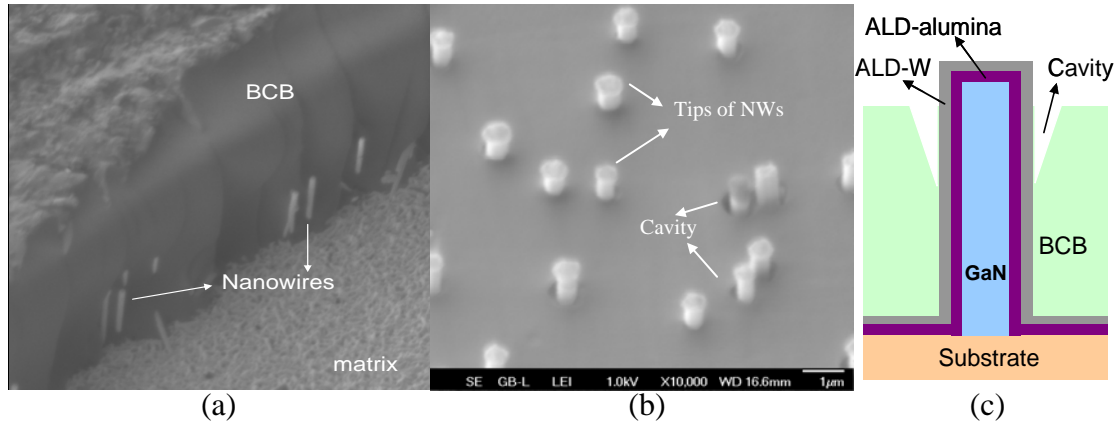


Figure 4: BCB encapsulation process for vertical GaN NWs. (a) GaN NWs were buried in thick BCB by dripping. (b) Mechanical polishing was employed to reduce thickness of BCB and tips of NWs were then exposed after RIE process. (c) Schematic drawing of cavity shown in (b). Scale bar in (b): 1 μm.

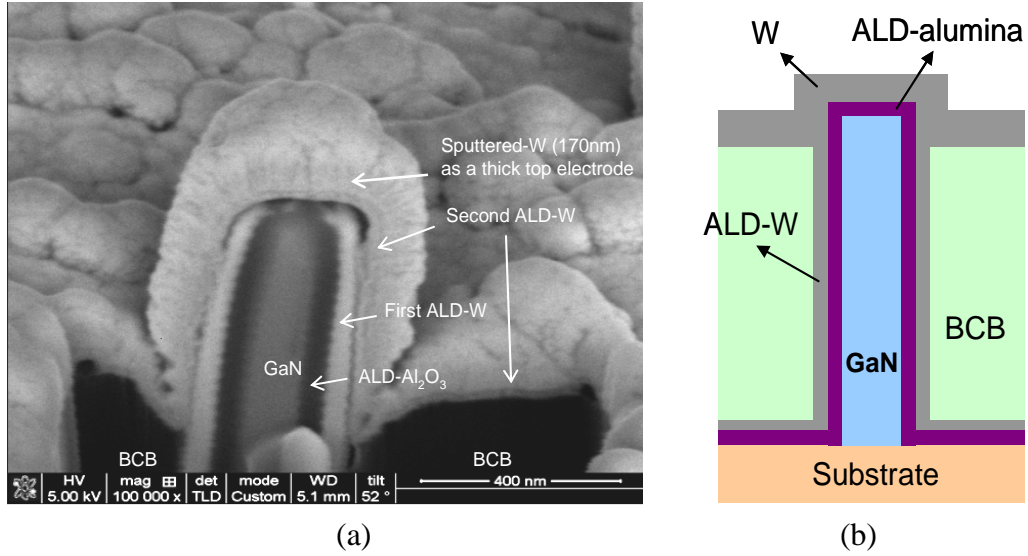


Figure 5: (a) Cross-sectional view of NW with ALD layers after FIB cutting. Scale bar: 400nm. (b) The corresponding schematic drawing. Second ALD-W was deposited for conformal coverage in the cavities. Sputtered-W with a thickness of 170nm was deposited after second ALD as a thick top electrode.

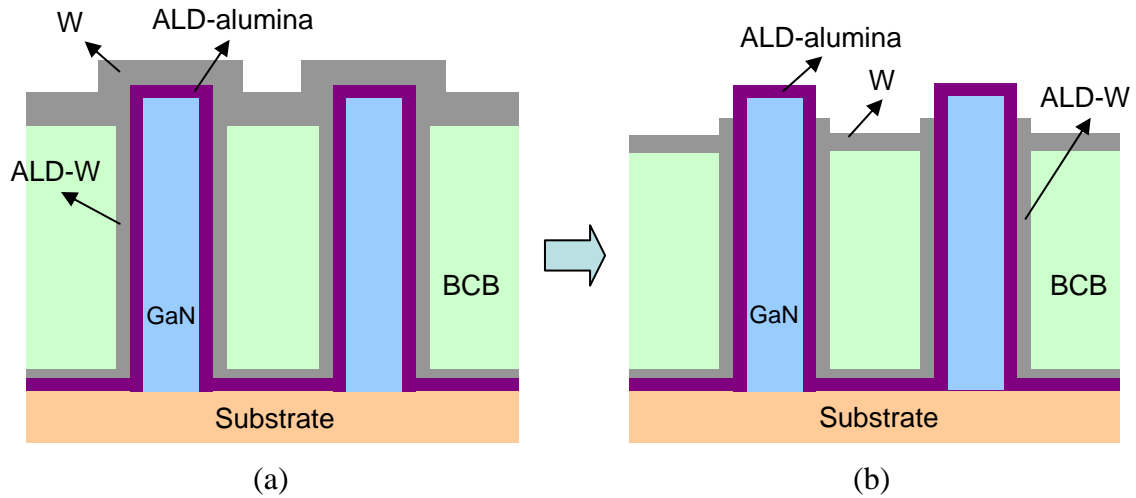


Figure 6: Schematic drawing of (a) nanowires interconnected with tips covered, and (b) nanowires interconnected with tips exposed after the local interconnect process. Photoluminescence signal can be generated and measured after W at tips is locally removed.

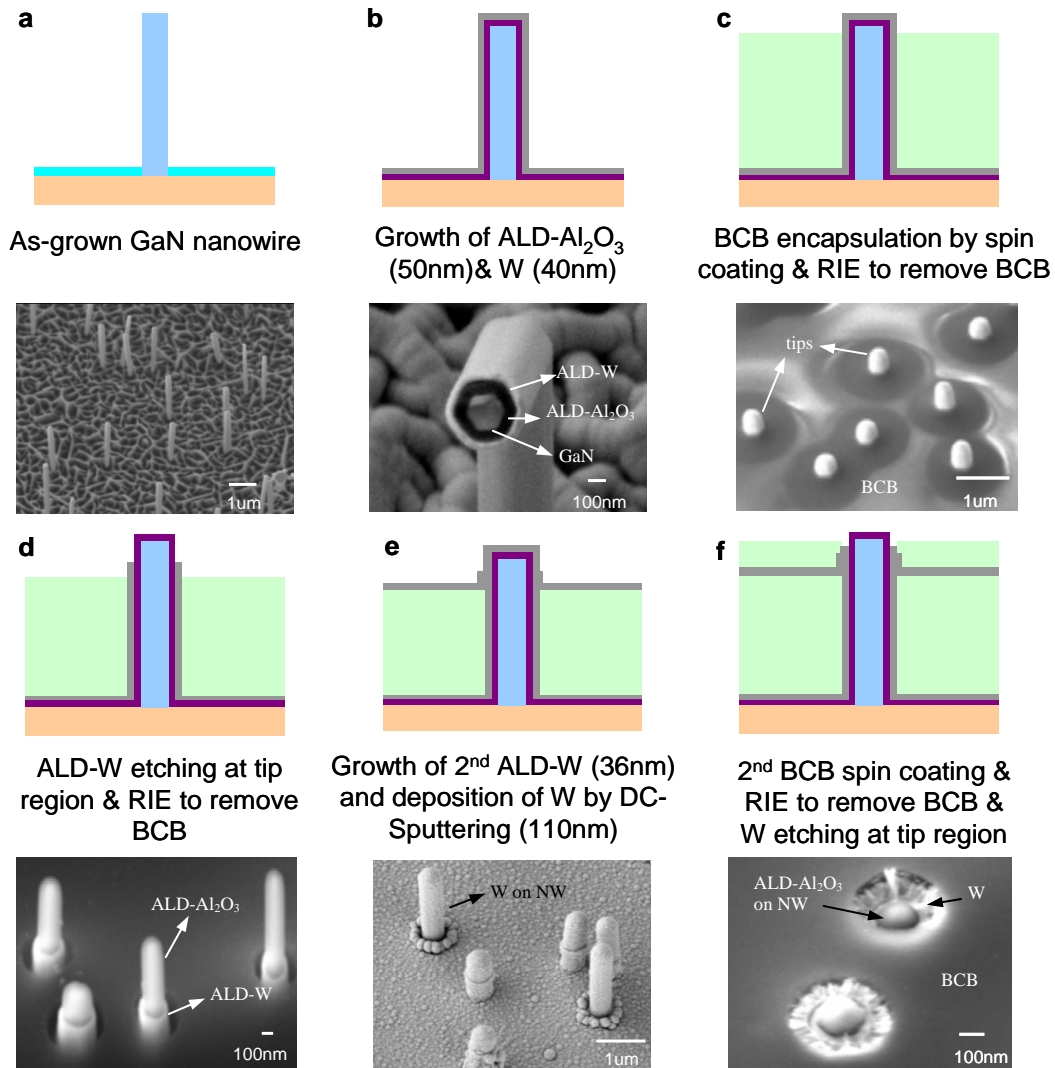
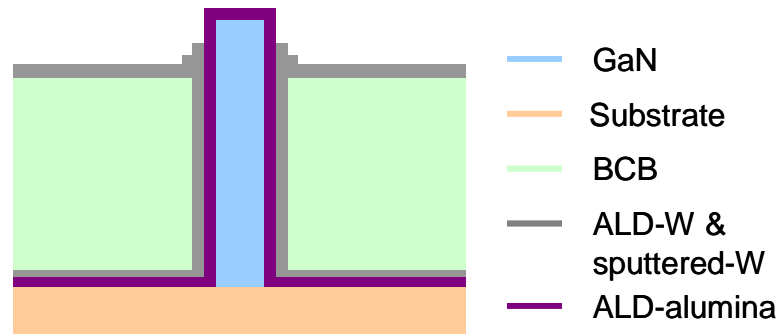


Figure 7: Fabrication process flow and corresponding experimental results of a local interconnect process that results in nanowires interconnected with tips exposed (no W-layer on the NW tip).



RIE to totally remove 2<sup>nd</sup> BCB

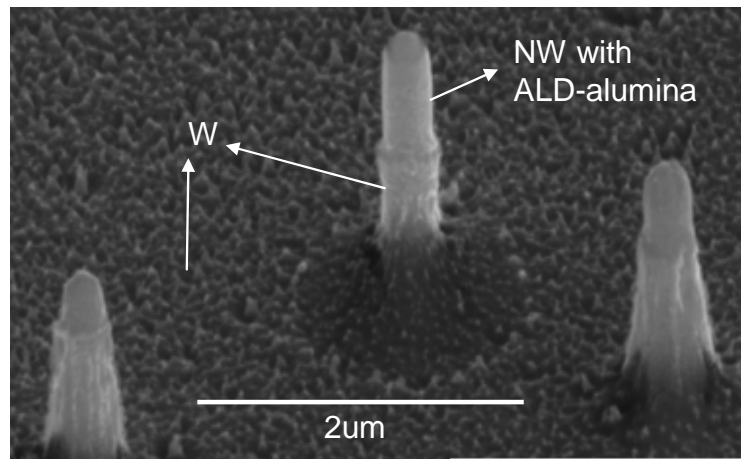
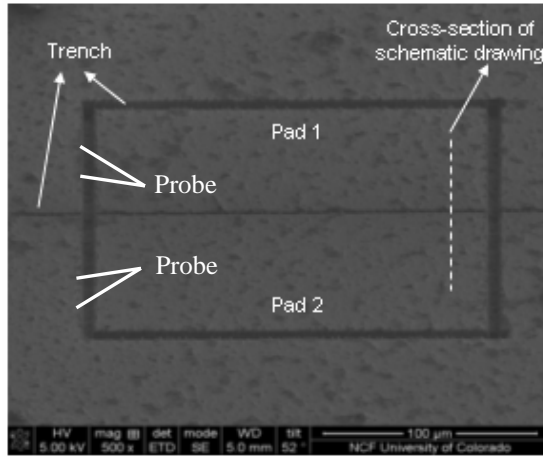
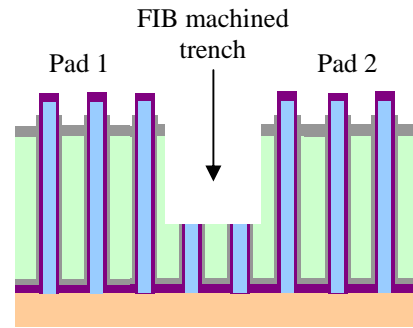


Figure 8: (top) Schematic drawing of final step of local interconnect process and (bottom) SEM image of GaN NWs with tip exposed (no W on tip region) after local interconnect process.



(a)



(b)

Figure 9: (a) SEM image of trenches fabricated by FIB and (b) schematic drawing of cross-sectional view. Trenches were fabricated by FIB cutting to isolate pad 1 and pad 2. The dimension of each pad is 200um (width) x 100um (length). The depth of trenches is 3um.

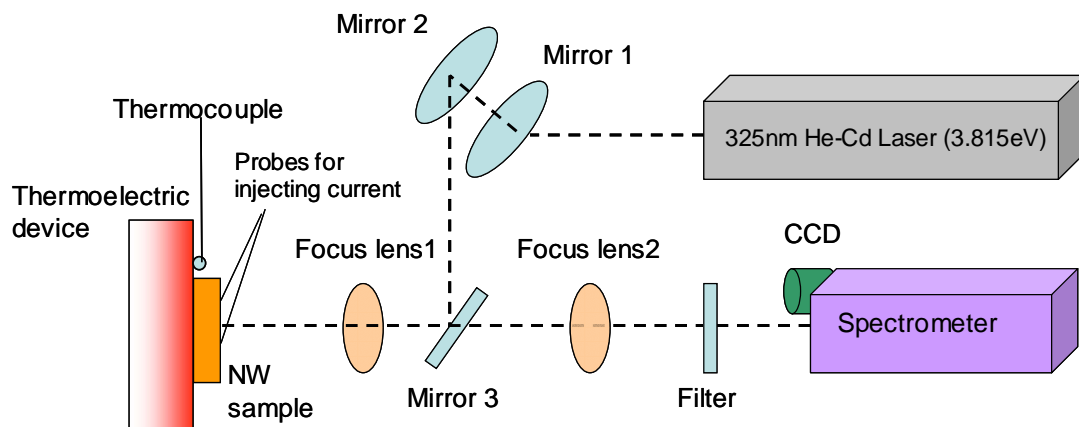


Figure 10: Experimental setup of PL measurement. Probes were respectively positioned on pads of NW sample under optical microscope to provide current into W interconnect. The laser spot diameter is around 13 $\mu$ m. Average number of NWs shined by laser is 10 by FESEM examination.

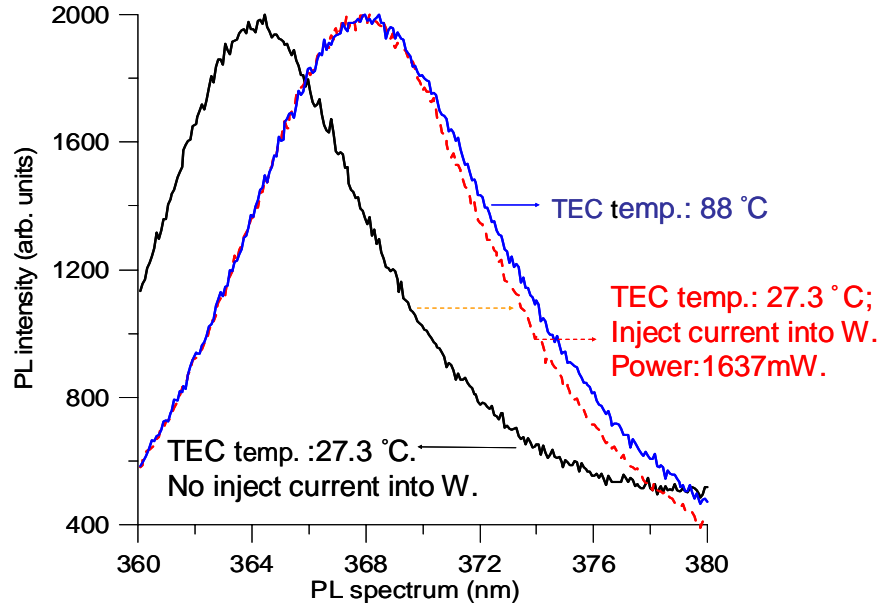


Figure 11: Experimental results of PL tuning by using TEC to heat NWs (solid line in blue) and by injecting current into W interconnect to heat NWs (dash line in red). The connection of W interconnect on NWs was confirmed by current injection into W interconnect to tune PL wavelength. The difference in PL slope could be due to the non-uniformity of the temperature distribution along the NWs under different heating mechanisms (TEC heating or current injection).

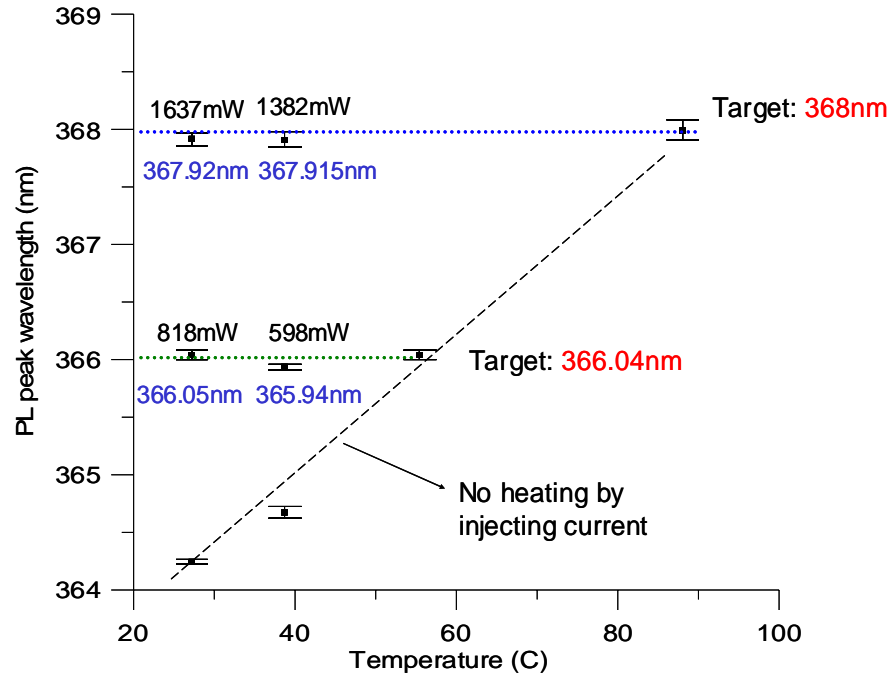


Figure 12: Experimental results of tunable PL wavelength by heating. PL peak wavelength of NW array can be dynamically tuned to target wavelengths by changing the input power supplied to ALD-tungsten interconnect. PL peak wavelength is determined by using the quadratic fit to the neighboring data of raw peak.

## Biographies

**Jen-Hau Cheng** received his B.S. degree in mechanical engineering from Tamkang University, Taiwan in 2000 and his M.S. degree in engineering and system science from National Tsing Hua University, Taiwan in 2002. He worked as a design engineer in the center of Advanced Microsystems and Packaging Technology in Industrial Technology Research Institute (ITRI) in Taiwan from 2002 to 2005. He is currently a mechanical engineering Ph.D student at the University of Colorado at Boulder. His research interests include interconnect and packaging for nanowires.

**Dragos Seghete** received his B.S. degree with honors in chemistry and mathematics from University of Arkansas, Fayetteville, AR in 2005. He is currently a physical chemistry Ph.D. student at the University of Colorado at Boulder. His research interests include the exploration of new chemistries for the atomic and molecular layer deposition of low density materials and the development of new applications for existing ALD and MLD systems.

**Myongjai Lee** majored mechanical engineering in Korea (Hongik University for B.S. and KAIST for M.S.) and USA (University of Colorado at Boulder for Ph.D.). His research interests include the nano-structured materials and N/MEMS devices for the applications in energy area.

**John Schlager** received the B.A. degree in physics and mathematics from Lawrence University, Appleton, WI, in 1985 and the M.S. and Ph.D. degrees in physics from the University of Colorado, Boulder, CO, in 1987 and 1992, respectively. He has been a member of the Optoelectronics Division at the National Institute of Standards and Technology since May 1987 where he has been researching mode-locked fiber lasers, optical sampling measurements, fiber nonlinearities, multimode fiber characterization, and mode-locked glass waveguide lasers. He is currently characterizing nano-scale semiconductors using optical methods. Dr. Schlager is a member of the IEEE, and Phi Beta Kappa.

**Kris A. Bertness** is a physicist in the Optoelectronics Division of the National Institute of Standards and Technology in Boulder, CO. Her technical focus has been on III-V semiconductor crystal growth, characterization, and device design, with particular emphasis on nanowires and quantum dots. NIST's recent work GaN nanowires was recognized with an R&D Magazine MicroNano 25 Award in 2006. Prior to joining NIST in 1995, she developed record-efficiency solar cells with a team at the National Renewable Energy Laboratory. She received her Ph. D. in Physics from Stanford University.

**Norman A. Sanford** is the Project Leader of the Optoelectronic Materials Metrology effort at the National Institute of Standards and Technology, Boulder, CO. He received the Ph.D. in Physics from Rensselaer Polytechnic Institute in 1983 for studies in nonlinear magneto-optics that were jointly performed with GTE Laboratories, Waltham, MA. He was with Sperry Research Center, Sudbury, MA, and Polaroid Corporation,

Cambridge, MA, and pursued fiber optics, sensors, integrated optics, nonlinear optics, and solid state waveguide lasers at these laboratories. Since joining NIST in 1988, he has worked on characterization of rare-earth doped glasses and ferroelectrics, waveguide lasers, nonlinear optics, and characterization of wide-bandgap III-nitride materials and nanowires. Sanford is a Fellow of the Optical Society of America and served as an Associate Editor of the Journal of Quantum Electronics for several years. He has authored or co-authored roughly 100 publications, 2 invited book chapters, and holds 14 U.S. patents.

**Ronggui Yang** is the Sanders Faculty Fellow in engineering and an assistant professor of Mechanical Engineering at the University of Colorado at Boulder. Dr. Ronggui Yang received his Ph.D degree focusing on nanoscale energy transport from MIT in February 2006, a MS in MEMS from UCLA in 2001, a MS in Thermal Engineering from Tsinghua University in 1999 and a BS in Thermal Engineering from Xi'an Jiaotong University in 1996. His research interests are on the application of micro/nano- technologies for large-scale energy conversion, storage and transport. Dr. Yang authored and co-authored more than 30 journal papers and has delivered more than 40 invited talks and seminars. His innovative research has won him many awards including the NSF CAREER Award in 2009, Technology Review's TR35 Award in 2008, the DARPA/MTO Young Faculty Award (YFA) in 2008, the Goldsmid Award from the International Thermoelectrics Society in 2005, and a few Best Research Paper Award and nominations from the ASME and IEEE.

**Steven M. George** is Professor in the Department of Chemistry and Biochemistry and Department of Chemical and Biological Engineering at the University of Colorado at Boulder. Dr. George received his B.S. in Chemistry from Yale University (1977) and his Ph.D. in Chemistry from the University of California at Berkeley (1983). He has more than 250 peer-reviewed publications in the areas of thin film growth, surface science and physical chemistry. Dr. George is a Fellow of the American Vacuum Society (2000) and a Fellow of the American Physical Society (1997). Dr. George's research interests are in the areas of surface chemistry, thin film growth and nanostructure engineering. He is currently directing an internationally recognized research effort focusing on atomic layer deposition (ALD) and molecular layer deposition (MLD). This research is examining new surface chemistries for ALD and MLD growth, measuring thin film growth rates, characterizing the properties of thin films and developing new reactors for film growth. Dr. George served as Chair of the first American Vacuum Society (AVS) Topical Conference on Atomic Layer Deposition (ALD 2001) held in Monterey, California. He also teaches a one-day short course on ALD for the AVS. In addition, Dr. George is a co-founder of ALD NanoSolutions, Inc., a startup company that is working to commercialize ALD technology.

**Y. C. Lee** is a Professor of Mechanical Engineering at the University of Colorado, Boulder. He received his B.S. degree in Mechanical Engineering from the National Taiwan University in 1978, and his M.S. (1982) and Ph.D. (1984) degrees from the University of Minnesota. Dr. Lee is the Director of DARPA Center on Nanoscale Science and Technology for Integrated Micro/Nano-Electromechanical Transducers (iMINT) at

the University of Colorado - Boulder. He is also the Administrative Director of the Nanomaterials Characterization Facility. Prior to joining the University, he was at AT&T Bell Laboratories, Murray Hill, New Jersey. Dr. Lee's research is on the integration of microelectromechanical systems (MEMS), nanoelectromechanical systems (NEMS) and microelectronic, optoelectronic and microwave devices. He has published over 200 papers in journals and conferences. Dr. Lee was an Associated Editor of ASME Journal of Electronic Packaging (2001-2004) and a Guest Editor for special issues on Packaging for Micro/Nano-Scale Systems for IEEE Transaction on Advanced Packaging (2003, 2005 and 2007). He is an ASME Fellow and has received the following awards: Presidential Young Investigator (NSF, 1990); Outstanding Young Manufacturing Engineer Award (SME, 1992); Outstanding Paper Award (IEEE-ECTC, 1991); Outstanding Paper Award (ASME J. of Electronic Packaging, 1993); Honorable Mention Paper Award (IEEE Transactions on Advanced Packaging, 2003); Meritorious Paper Award (GOMACTech-03); CU-ME Woodward Outstanding Mechanical Engineering Faculty Award, 2005-2006; and ASME Electronic and Photonic Packaging Division's Mechanics Award in 2007.